ACS SyntheticBiology

Research Article

pubs.acs.org/synthbio

SoxR as a Single-Cell Biosensor for NADPH-Consuming Enzymes in *Escherichia coli*

Solvej Siedler,[†] Georg Schendzielorz, Stephan Binder, Lothar Eggeling, Stephanie Bringer, and Michael Bott*

IBG-1: Biotechnology, Institute of Bio- and Geosciences, Forschungszentrum Jülich, D-52425 Jülich, Germany

Supporting Information

ABSTRACT: An ultra-high-throughput screening system for NADPH-dependent enzymes, such as stereospecific alcohol dehydrogenases, was established. It is based on the [2Fe−2S] cluster-containing transcriptional regulator SoxR of *Escherichia coli* that activates expression of *soxS* in the oxidized but not in the reduced state of the cluster. As SoxR is kept in its reduced state by NADPH-dependent reductases, an increased NADPH demand of the cell counteracts SoxR reduction and increases *soxS* expression. We have taken advantage of these properties by placing the *eyfp* gene under the control of the *soxS* promoter and analyzed the response of *E. coli* cells expressing an NADPH-dependent alcohol dehydrogenase from *Lactobacillus brevis* (*Lb*Adh), which reduces methyl acetoacetate to (*R*)-methyl 3-hydroxybutyrate. Under suitable conditions, the specific fluorescence of the cells correlated with the substrate concentration added and with *Lb*Adh enzyme activity, supporting the NADPH responsiveness of the sensor. These properties enabled sorting of single cells harboring wild-type *Lb*Adh from those with lowered or without *Lb*Adh activity by fluorescence-activated cell sorting (FACS). In a proof-of-principle application, the system was used successfully to screen a mutant *Lb*Adh library for variants showing improved activity with the substrate 4-methyl-2-pentanone.

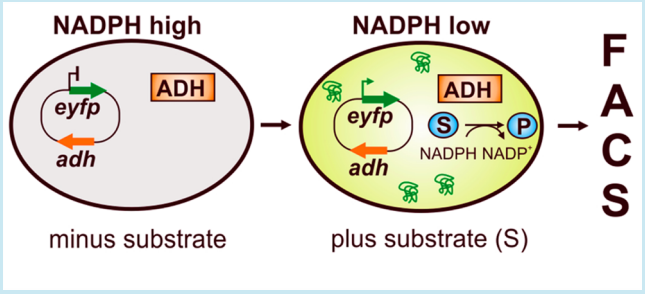

KEYWORDS: *NADPH biosensor, alcohol dehydrogenases, enzyme evolution, single-cell analysis, FACS*

Redox reactions are at the core of cellular metabolic processes, and about one-quarter of known enzymes are oxidoreductases.[1] A feature of many of these enzymes is their stereo- and regiospecificity. The pharmaceutical industry takes advantage of these properties as well as the mild and environmentally friendly conditions under which enzyme-catalyzed reactions proceed. Among such processes, alcohol dehydrogenases are of particular interest.[2,3] They are employed in the reduction of various ketones to produce enantiopure secondary alcohols. These enzymes are frequently NADPH-dependent, and there is a need for a continuous supply of the reduced cofactor for the reaction to proceed.[2,4,5] This applies both for isolated enzymes and for whole-cell processes.[6,7]

In our studies with *Escherichia coli* on the reductive biotransformation of methyl acetoacetate (MAA) to (*R*)-methyl 3-hydroxybutyrate (MHB) by a strictly NADPH-dependent alcohol dehydrogenase from *Lactobacillus brevis* (*Lb*Adh),[6,8,9] we noticed a significantly increased mRNA level of the *soxS* gene in cells catalyzing MAA reduction. SoxS is a transcription factor whose expression is activated under conditions of oxidative stress by SoxR.[10−13] The genes of the SoxRS regulon mediate the cellular response to superoxide, to diverse redox-cycling drugs like paraquat, or to nitric oxide.[14,15] SoxR is a homodimer with each subunit containing an [2Fe−2S] cluster.[16,17] Only when the cluster is oxidized to $[2Fe-2S]^{2+}$ is transcriptional activity conferred to SoxR, which in turn results in the expression of *soxS*.[18,19] SoxS then activates expression of the SoxRS regulon, which includes, for example, the genes for superoxide dismutase (*sodA*), glucose 6-phosphate dehydrogenase (*zwf*), or fumarase C (*fumC*).[20] Inactivation of SoxR involves its NADPH-dependent reduction catalyzed by the *rsxABCDGE* and *rseC* products.[21]

The nature of the cellular signal sensed by SoxR is still a matter of debate.[22−24] Besides direct oxidation of the iron−sulfur centers by superoxide[25] and redox cycling drugs,[23] Liochev and Fridovich first suggested that the SoxRS regulon is responsive to the NADPH/$NADP^+$ ratio,[26] which was supported by several studies. Krapp et al.[27] showed that introduction of a heterologous $NADP^+$-reducing enzyme, the nonphosphorylating glyceraldehyde 3-phosphate dehydrogenase from wheat, into *E. coli* led to an increased NADPH/$NADP^+$ ratio, inhibition of the SoxR-mediated response, and enhanced sensitivity to the superoxide propagator methyl viologen (MV) and vice versa: overproduction of pea ferredoxin, which stimulates NADPH oxidation via ferredoxin-NADP(H) reductase, led to a decreased NADPH/$NADP^+$ ratio, triggering of the SoxR response and a higher tolerance to MV. Kobayashi and Tagawa[28] isolated an 84 kDa enzyme that catalyzed the NADPH-dependent reduction of oxidized SoxR.

Received: August 14, 2013
Published: November 27, 2013

In our previous work, we showed that after starting the NADPH-dependent reductive biotransformation of MAA to MHB the NADPH/NADP$^+$ ratio of the cells decreased, whereas the NADH/NAD$^+$ ratio (and the *soxS* mRNA level) increased.[29] These results favor NADPH and disfavor NADH as a SoxR reductant. In the present work, we provide further evidence that SoxR can sense NADPH availability, and we utilized this finding to develop a sensor for the in vivo analysis of NADPH-dependent reactions, offering a number of exciting possibilities for high-throughput analysis and the development of NADPH-dependent enzymes.

RESULTS AND DISCUSSION

SoxR as an NADPH Sensor. Our previous studies indicated that the transcriptional regulator SoxR of *E. coli* activates expression of its target gene *soxS* during reductive biotransformations with a high demand of NADPH because of a reduced capability of the cell for NADPH-dependent reduction and inactivation of SoxR. On the basis of this correlation, SoxR might be used as an NADPH sensor. To evaluate and apply such a function of SoxR, we constructed plasmid pSenSox in which *soxR* of *E. coli* DH5α together with the *soxR*–*soxS* intergenic region and a small part of the *soxS* coding region followed by a stop codon were cloned in front of *eyfp*, thereby placing synthesis of the autofluorescent protein eYFP under transcriptional control of the *soxS* promoter (Figure 1). The sensor plasmid also encodes the NADPH-dependent alcohol dehydrogenase of *L. brevis*, *Lb*Adh, under the control of an isopropyl β-D-thiogalactoside-inducible promoter. *Lb*Adh was previously shown by us and others to convert efficiently MAA stoichiometrically to MHB.[6,8,29,30]

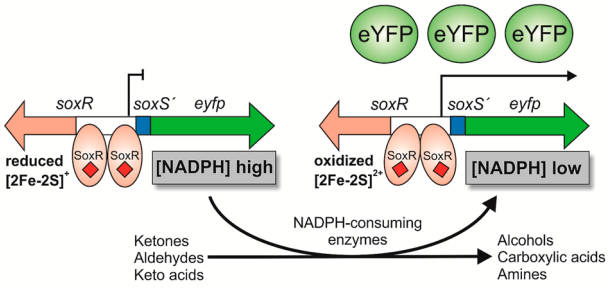

Figure 1. NADPH biosensor based on the transcriptional regulator SoxR of *E. coli*. Dimeric SoxR with two Fe–S clusters binds to the *soxR*–*soxS* intergenic region. At sufficient NADPH levels, the Fe–S clusters are kept in the reduced state, and SoxR is inactive. The enhanced activity of NADPH-consuming enzymes impedes SoxR reduction, and the oxidized Fe–S clusters trigger a conformational change of SoxR, causing transcription of its target gene *soxS*. In the NADPH biosensor pSenSox, *soxS* has been replaced by *eyfp* coding for the fluorescent protein eYFP, which allows for the identification of cells with a low NADPH level by their increased fluorescence.

E. coli BL21(DE3) was transformed with plasmid pSenSox and used for whole-cell biotransformation assays in 2× TY medium with 10–70 mM MAA as an *Lb*Adh substrate. Complex medium was used to enable eYFP synthesis. In these assays, NADPH is provided by the metabolism of components present in yeast extract and tryptone. For online recording of eYFP fluorescence and growth, a BioLector system was used. Under the chosen conditions, at best doubling of the cells was observed (Figure S1). Upon addition of MAA, the cultures started to emit fluorescence with the initial slope of the fluorescence increase being independent of the MAA concentration added (Figure 2a). As recently discussed by us,[30] in the biotransformation system used here with a high activity of wild-type *Lb*Adh, the enzyme is saturated with the substrate MAA, and metabolic NADPH generation is likely the limiting step. Increasing concentrations of MAA led to higher fluorescence maxima, and the time period required to reach these maxima also increased (Figure 2a). The maximal fluorescence intensity obtained for different initial MAA concentrations remained constant for several hours because of the marginal growth of the cells, the slow maturation kinetics of the eYFP chromophore, and the high stability of eYFP. When the specific fluorescence achieved after 10 h was plotted against the initial MAA concentration, an almost linear

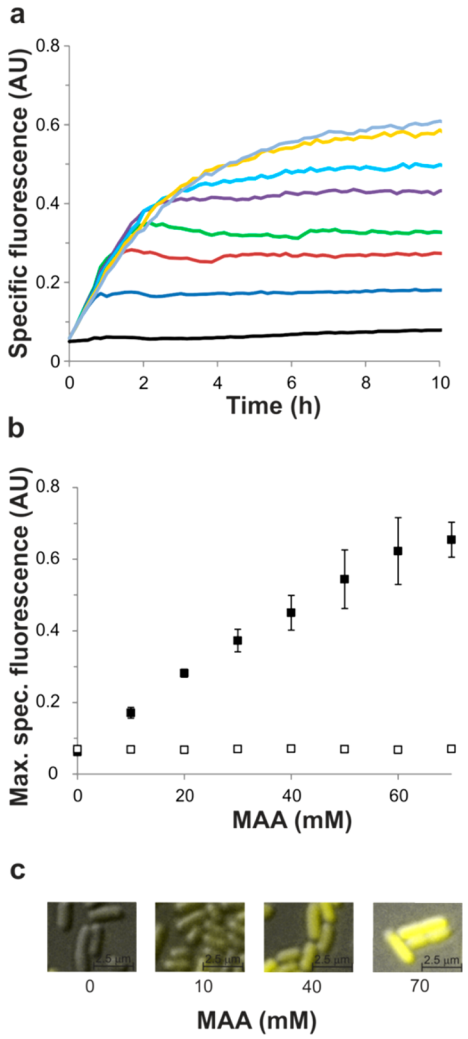

Figure 2. (a) Specific fluorescence (485 nm excitation, 520 nm emission) of *E. coli* carrying the NADPH biosensor pSenSox during biotransformation of 10 (dark blue), 20 (brown), 30 (green), 40 (purple), 50 (light blue), 60 (yellow), and 70 mM (gray) MAA to MHB via the NADPH-dependent alcohol dehydrogenase *Lb*Adh. A control without MAA is shown in black. (b) Specific fluorescence of cells (■) measured after 10 h of biotransformation plotted against the initial MAA concentration. Mean values and standard deviations of three independent replicates are shown. The empty squares (□) show the values obtained with the control plasmid, pSenNeg, encoding an inactive *Lb*Adh fragment. (c) Epifluorescence of cells from biotransformations with 0, 10, 40, or 70 mM MAA.

dx.doi.org/10.1021/sb400110j | *ACS Synth. Biol.* 2014, 3, 41–47

Table 1. Dependence of the Maximal Specific Fluorescence from the Specific *Lb*Adh Activity of Cells

plasmids carried in *E. coli* BL21(DE3)	IPTG[a]	*Lb*Adh activity (μmol min^{-1} (mg protein)$^{-1}$)[b]	maximal specific fluorescence[b,c]
pSenNeg	−	0.03 ± 0.01	0.07 ± 0.01
pSenSox pET28a[d]	−	0.5 ± 0.1	0.09 ± 0.01
pSen-L194S	−	0.7 ± 0.3	0.11 ± 0.01
pSen-L194A	−	2.7 ± 0.6	0.18 ± 0.04
pSenSox	−	6.3 ± 0.6	0.38 ± 0.02
pSenSox	+	15.2 ± 2.0	0.46 ± 0.04

[a]IPTG was added at 1 mM. To allow reproducible expression, plasmid pSenSox carries no *lacI* gene, but *E. coli* BL21(DE3) contains a chromosomal copy of *lacI*. IPTG was used to maximize expression. [b]Mean values and standard deviations from three replicates are given. [c]Values were measured after 19 h of biotransformation with 40 mM MAA. [d]Vector pET28a provided an additional copy of *lacI* for stronger repression of *Lbadh*.

relationship was obtained for MAA concentrations up to 60 mM (Figure 2b). In the absence of MAA, constant background fluorescence was observed. Similarly, in biotransformation experiments with cells carrying plasmid pSenNeg encoding an inactive *Lb*Adh fragment, only background fluorescence was detectable independent of the MAA concentration added. These controls confirm that the fluorescence increase was strictly dependent on the NADPH-dependent reduction of MAA to MHB. The increased fluorescence obtained with increased MAA concentrations was also visible at the single-cell level by epifluorescence microscopy (Figure 2c) and flow cytometry (see below).

The results reported above support the view that SoxR of *E. coli* is active under conditions of high NADPH demand, as obtained by the reduction of MAA to MHB by *Lb*Adh. By measuring SoxR activity via *eyfp* expression under control of the *soxS* promoter, we showed that the maximal specific fluorescence of cells correlates with the concentration of MAA reduced to MHB (Figure 2). To explain the observed correlation, we propose that SoxR is subject to permanent oxidation under aerobic conditions (e.g., by superoxide ions, which were reported to be formed at a rate of 5 μM s^{-1}),[15,31] but it is kept in its reduced form by NADPH-dependent reduction via the *rsxABCDGE* and *rseC* gene products. Under conditions of high NADPH demand, SoxR reduction is hampered, thus favoring the presence of oxidized, active SoxR. Regarding the discussion on the nature of the signal sensed by SoxR, our data support the concept of Liochev and Fridovich[26] that there are multiple ways to induce the SoxRS regulon, which ultimately shift the equilibrium of oxidized and reduced SoxR to the oxidized form. This can either happen by increasing the oxidation of reduced SoxR or by decreasing the reduction of oxidized SoxR, as exemplified in our study.

Correlation between Fluorescence and *Lb*Adh Activity. In the next series of experiments, the influence of varying *Lb*Adh activities on the fluorescence output was tested (Table 1). For this purpose, six cultures with a specific *Lb*Adh activity between 0.03 U (mg protein)$^{-1}$ (background activity) and 15.2 U (mg protein)$^{-1}$ were used in biotransformations with a set of different MAA concentrations. The different *Lb*Adh activities were achieved either by varying the expression level of the wild-type enzyme via induction with IPTG or repression with LacI or by using mutant *Lb*Adh proteins with amino acid exchanges Leu194Ser or Leu194Ala. The time course of specific fluorescence for these cultures when incubated with different MAA concentrations is shown in Figure S2. Higher *Lb*Adh activities led to higher maximal specific fluorescence, and this is shown exemplarily for 40 mM MAA in Table 1. Thus, the pSenSox system in the living cell offers the possibility to distinguish NADPH-dependent enzymes with varying specific activity.

Application of SoxR for High-Throughput Screening of NADPH-Dependent Enzymes. Recently, metabolite-activated transcription factors controlling *eypf* expression were used to monitor the cytosolic concentration of the respective metabolites in single bacterial cells, which allowed high-throughput screening and isolation of single producer cells using fluorescence-activated cell sorting (FACS).[32−34] On the basis of these results, we tested whether single cells differing in their specific *Lb*Adh activity also can be analyzed and sorted via FACS. For this purpose, *E. coli* cells carrying either pSenSox (6.2 U mg^{-1} *Lb*Adh activity), pSen-L194A (2.7 U mg^{-1}), or pSenNeg (0.03 U mg^{-}1) were used for biotransformation of 70 mM MAA for 19 h and then subjected to FACS. The resulting combined histogram (Figure 3a) shows three well-resolved peaks of eYFP fluorescence, indicating that the three strains differing in their specific *Lb*Adh activities form homogeneous populations. Using an appropriate gate, P1, to exclude cells with background fluorescence (carrying pSenNeg), 80.8% of the population of cells with high fluorescence (carrying pSenSox) and 1.5% of the cells with lower fluorescence (carrying pSen-L194A) could be isolated.

These results encouraged us to test the suitability of pSenSox for high-throughput screening of alcohol dehydrogenase mutant libraries. To do this, we introduced mutations in *Lb*Adh both randomly by error-prone PCR and by individual site-directed mutagenesis at positions Ala93, Leu152, and Val195, which are known to be involved in substrate binding.[9] The cells of the four mutant libraries were pooled and used for reductive biotransformation of 20 mM 4-methyl-2-pentanone (4M2P). This prochiral ketone was chosen because the reduced product (*R*)-4-methyl-2-pentanol is of economic interest and because wild-type *Lb*Adh has only ∼12% activity with this substrate as compared to MAA (15.5 μmol min^{-1} (mg protein)$^{-1}$). Analysis of cells containing wild-type *Lb*Adh showed that the maximal specific fluorescence obtained with 20 mM 4M2P was obtained already after 2 to 3 h of biotransformation. Therefore, the cells of the mutant libraries were subjected to FACS after approximately 3 h of biotransformation.

We performed a sort on the library in which wild-type *Lb*Adh after biotransformation of 4M2P was used to define the lower bound of the sorting gate. This bound was set close to the maximal fluorescence of cells containing wild-type *Lb*Adh, which enhances the chances for identifying even slightly improved Adh variants but also for sorting false positives. The wild-type *Lb*Adh-containing strain served as a positive control after biotransformation of MAA instead of 4M2P (Figure 3b). In the scatter plots of wild-type *Lb*Adh with either 4M2P or

dx.doi.org/10.1021/sb400110j | ACS Synth. Biol. 2014, 3, 41−47

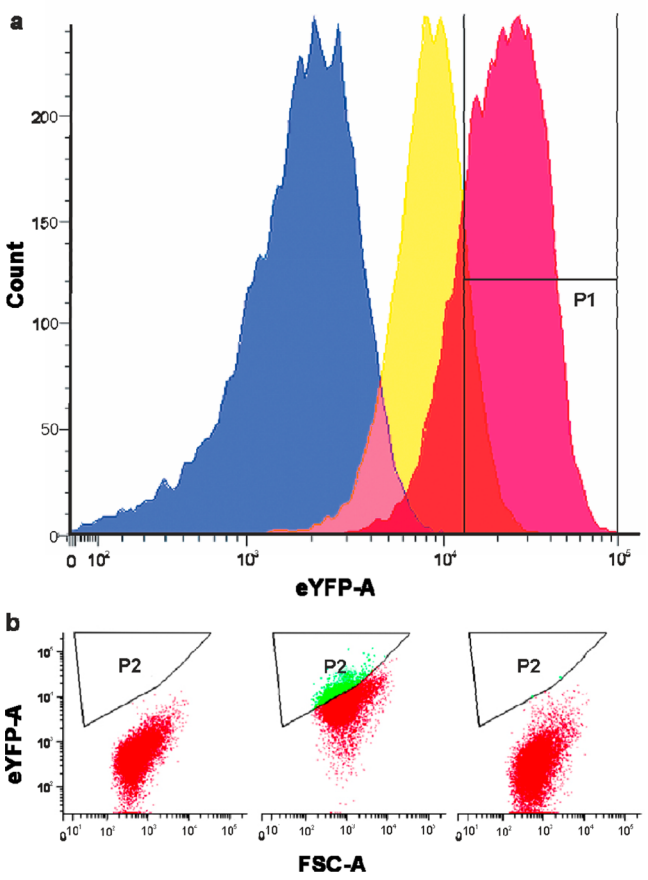

Figure 3. Flow cytometric analysis of *E. coli* cells with the *soxR*−*soxS*-based NADPH sensor and different NADPH-dependent *Lb*Adh activities. (a) Combined fluorescence histograms of three *E. coli* strains carrying either pSenNeg (blue, 0.03 U mg^{-1} *Lb*Adh acitivity), pSen-L194A (yellow, 2.7 U mg^{-1} *Lb*Adh activity), or pSenSox (red, 6.28 U mg^{-1} *Lb*Adh activity) after biotransformation for 19 h with 70 mM MAA. Gate P1 was used for differentiation of pSenNeg and mutant or wild-type populations. (b) FACS-generated scatter plots displaying the forward scatter signal (FSC) and the eYFP signal of *E. coli* cells carrying pSenSox after reductive biotransformation of 20 mM 4M2P (left side) or 20 mM MAA (middle). On the right side, the library of mutant *Lb*Adhs was used for biotransformation of 20 mM 4M2P and then subjected to FACS. Gate P2 was used for mutant screening.

MAA as a substrate, a relatively broad distribution of the cells was observed. Similar observations were made for yeast cells with a theophylline sensor,[35] and the authors speculated that individual gene expression noise was responsible for this heterogeneity, arising from cell-specific differences in cell cycle stage, fluctuations in plasmid copy numbers, and other parameters.[36] Such heterogeneity may distort the quantitative output of a metabolite sensor to some extent and enhance the background signal, thereby increasing the rate of false positives. In a single screen, 10^6 cells of the *Lb*Adh mutant library were analyzed, and 250 cells showing slightly enhanced fluorescence were selected and spotted on plates, of which 123 grew to form colonies. Ninety six of these clones were analyzed in a microtiter plate for fluorescence intensity after a 2 to 3 h incubation with 4M2P (Figure S3). From six selected clones with high specific fluorescence at the selected time point, the specific *Lb*Adh activity was determined (Table S1), and one clone was identified that had a 36% increased activity with the substrate 4M2P accompanied by an 8-fold increased K_m value (Table 2). The plasmid of this mutant clone was fully sequenced and found to contain a single mutation in the *Lbadh* gene that led to an Ala93Met exchange.

Table 2. Properties of Wild-Type *Lb*Adh and Variant *Lb*Adh-A93M for the Substrate 4-Methyl-2-pentanone

enzyme[a]	V_{max} (μmol min^{-1} mg^{-1})[b]	K_m (mM)[b]
*Lb*Adh	1.94 ± 0.02	0.11 ± 0.01
*Lb*Adh-A93M	2.62 ± 0.03	0.88 ± 0.07

[a]Enzyme activities were determined with crude extracts of the respective strains carrying either pSenSox or pSen-A93M. [b]Mean values and standard deviation from three replicates are given.

In conclusion, the correlation between NADPH consumption and fluorescence was visible at the single-cell level and suitable for FACS analysis, allowing the highest throughput assays currently possible. Because we could identify conditions leading to a good correlation between the specific activity of the NADPH-consuming enzyme and the specific fluorescence of the cells, the SoxR sensor provides a generalized high-throughput screening system for this type of enzymes. We demonstrated this potential by the rapid isolation of an *Lb*Adh variant via FACS with an improved activity toward the substrate 4M2P (Table 2). To reduce the number of false positives, suitable enrichments steps have to be identified and included in future applications of the SoxR-based sensor, as reported for other high-throughput screening systems.[35,37−39] As long as educts and products can enter and leave the sensor-containing cells, libraries of NADPH-dependent enzymes can now be assayed in a high-throughput format without the development of specific assays. This novel technology has the potential to expedite the availability of new enzymes for the synthesis of chiral compounds significantly.

METHODS

Bacterial Strains, Media, and Growth Conditions. Bacterial strains and plasmids are listed in Table 3. *E. coli* strains were transformed by the method described by Hanahan[40] and cultivated in LB medium[41] or in 2× YT medium (16 g L^{-1} of tryptone, 10 g L^{-1} of yeast extract, and 5 g L^{-1} of sodium chloride). *E. coli* DH5α[40] was used for cloning and screening purposes, and *E. coli* BL21 Star (DE3) (Invitrogen, Karlsruhe, Germany) and derivatives were used for gene expression and whole-cell biotransformation for sensor establishment. Plasmids were selected by adding antibiotics to the medium at a final concentration of 100 μg mL^{-1} of ampicillin (pSenSox and derivatives) and 50 μg mL^{-1} of kanamycin (pET28a).

Recombinant DNA Work. Standard methods, including PCR and DNA restriction or ligation, were carried out according to standard protocols.[42] Oligonucleotides were synthesized by Biolegio eV (Nijmegen, The Netherlands) and are listed in Table 3. For construction of the plasmid-based biosensor pSenSox, the *E. coli* DNA region encompassing the *soxR* open reading frame, the *soxR*−*soxS* intergenic region, and the first 21 codons of *soxS* were amplified with Phusion DNA polymerase (Thermo Scientific) from chromosomal DNA of *E. coli* BL21(DE3) by PCR using oligonucleotides SoxS_for_*Sph*I and SoxR_rev_*Sal*I, which introduce *Sph*I and *Sal*I restriction sites as well as a stop codon after codon 21 of *soxS*. Additionally, the *eyfp* gene was amplified by PCR with

dx.doi.org/10.1021/sb400110j | *ACS Synth. Biol.* 2014, 3, 41−47

Table 3. Strains, Plasmids, and Oligonucleotides Used in This Work

strains, plasmids, and oligonucleotides	relevant characteristics or 5′−3′ sequence	ref or restriction site
Strains		
Escherichia coli BL21 Star (DE3)	F^- *ompT* $hsdS_B(r_B^-, m_B^-)$ *gal dcm rne*131 (DE3)	Invitrogen
Escherichia coli DH5α	F^- Φ 80Δ*lacZ*ΔM15 Δ(*lacZYA-argF*) U169 *deoR recA*1 *endA*1 *hsdR*17 (rk^-, mk^+) *phoA supE*44 λ^- *thi*-1 *gyrA*96 *relA*1	Hanahan[40]
Plasmids		
pBTac-*Lbadh*	Amp^R; pBtac1 derivative with *adh* gene from *Lactobacillus brevis*	Ernst et al.[8]
pSenSox	Amp^R; pBtac-*Lbadh* derivative containing *soxRS*-based biosensor	this study
pSenNeg	Amp^R; pSenSox derivative encoding an inactive *Lb*Adh fragment	this study
pSen-L194S	Amp^R; pSenSox derivative encoding *Lb*Adh-L194S	this study
pSenL194A	Amp^R; pSenSox derivative encoding *Lb*Adh-L194A	this study
pSenA93M	Amp^R; pSenSox derivative encoding *Lb*Adh-A93M	this study
pET28a	Kan^R; plasmid used for provision of IPTG-inducible *lacI* gene	Novagen
pSenLys	Kan^R; pJC1 derivative containing *lysGE*-based biosensor	Binder et al.[32]
Oligonucleotides[a]		
SoxS_for_*Sph*I	ATCTGCATGC***TTA***CGGCTGGTCAATATGCTCGTC	*Sph*I
SoxR_rev_*Sal*I	GCTAGTCGACCAAACTAAAGCGCCCTTGTG	*Sal*I
EYFP_for_*Sph*I	AGAGGCATGCAAGGAGAATTAC***ATG***GTGAGCAAGGGCGAGG	*Sph*I
EYFP_rev_*Cla*I	GCGCATCGATTTATTACTTGTACAGCTCGTCCATG	*Cla*I
ADH_negK_for	ACAAGAATTCGCTAAGAGTGTCGGCACTCC	*Eco*RI
ADH_negK_rev	GGCCAAGCTTCCGAAGAAGACACCATCAAG	*Hin*dIII
Ala93_for	GTTAATAACGCTGGGATCNNKGTTAACAAGAGTGTC	
Ala93_rev	GACACTCTTGTTAACMNNGATCCCAGCGTTATTAAC	
Leu152_for	GATCCTAGCTTAGGGGCNNKCAACGCATC	
Leu152_rev	GATGCGTTGMNNGCCCCTAAGCTAGGATC	
Val195_for	GACACCATTGGNNKATGACCTACCAGGGGC	
Val195_rev	GCCCCTGGTAGGTCATCAACMNNTGGTGTC	
ADH_mut_for	ATACGAATTC***ATG***TCTAACCGTTTGGATGG	*Eco*RI
ADH_mut_rev	GTGTGAAGCTT***A*CTA***TTGAGCAGTGTAG	*Hin*dIII

[a]Restriction sites are underlined, coding sequences are shown in italics, and start or stop codons are shown in bold.

oligonucleotides EYFP_for_*Sph*I, containing a ribosome binding site, and EYFP_rev_*Cla*I using the vector pSenLys[32] as template, thereby introducing restriction sites for *Sph*I and *Cla*I digestion. Both PCR products were cloned into the plasmid pBtac*Lbadh*,[8] resulting in plasmid pSenSox. For the construction of pSenNeg, a 221 bp region of the *adh* gene of *L. brevis* was amplified with the oligonucleotides ADH_negK_for and ADH_negK_rev, introducing *Eco*RI and *Hin*dIII restriction sites. The PCR product was cut with *Eco*RI and *Hin*dIII and used to replace the functional *adh* gene in plasmid pSenSox by a nonfunctional *adh* fragment. For individual saturation mutagenesis of codons Ala93, Leu152, and Val195 within the intact *adh* gene, the oligonucleotide pairs Ala93_for/Ala93_rev, Leu152_for/Leu152_rev, and Val195_for/Val195_rev were used according to the Stratagene site-directed mutagenesis kit with the following modifications: *Dpn*I (Fermentas) and PFX polymerase (Invitrogen) were used. For random mutagenesis of the entire *adh* gene, error-prone PCR (ep-PCR) was performed using the oligonucleotide pair ADH_mut_for/ADH_mut_rev, plasmid pSenSox as template, and Phusion DNA polymerase using the protocol described by Wilson and Keefe.[43] The PCR products were cut with *Eco*RI and *Hin*dIII and used to replace the native *adh* gene in pSenSox.

Whole-Cell Biotransformation in Microtiter Plates. For biotransformation experiments with *E. coli* cells harboring pSenSox or a derivative, 5 mL of 2× YT medium containing the appropriate antibiotic(s) was inoculated with a single colony of the respective strain and incubated overnight at 37 °C and 130 rpm. These precultures were used for inoculation of the main cultures to an optical density at 600 nm (OD_{600}) of 0.05. Main cultures were grown in 50 mL of 2× YT medium in the presence of the appropriate selection marker at 37 °C and 130 rpm to an OD_{600} of 0.3, induced with 1 mM IPTG when required, and incubated for another 3 h to an OD_{600} between 5 and 6. For online monitoring of fluorescence during biotransformation, 900 μL portions of the cultures were transferred into 48-well microtiter Flowerplates, and the cultures were supplemented with 100 μL of the biotransformation substrate dissolved in water and incubated in a BioLector cultivation system (m2plabs GmbH, Aachen, Germany) at 30 °C and 1200 rpm (shaking diameter 3 mm). During cultivation, biomass was measured as scattered light intensity (620 nm, signal gain factor of 15). The eYFP fluorescence of the cultures was measured at an excitation wavelength of 485 nm and an emission wavelength of 520 nm (signal gain factor of 70). The specific fluorescence was calculated as the ratio of eYFP fluorescence/scattered light intensity (given in a.u.).[44]

Ninety-Six-Well Screening System. For screening ADH activity, *E. coli* DH5α was transformed with the pSenSox derivatives subjected to site-directed mutagenesis and plated on LB agar plates containing 100 μg mL^{-1} of ampicillin. Single colonies were inoculated into 200 μL of 2× YT medium in a 96-well plate and grown overnight at 37 °C and 800 rpm. For the main culture, 5 μL of the preculture was inoculated into 145 μL of 2× YT medium in a 96-well plate. After 5 h, 40 mM methyl acetoacetate (MAA) or 40 mM 4M2P was added to the cells, and the fluorescence and the OD_{600} was measured every hour for 4 h using a plate reader (TECAN, Infinite 200 PRO). The specific fluorescence was defined as the fluorescence per OD_{600}.

dx.doi.org/10.1021/sb400110j | *ACS Synth. Biol.* 2014, 3, 41−47

Fluorescence Microscopy. Fluorescence microscopy was performed according to Mustafi et al.[33] Samples were placed on a microscope slide coated with a thin aqueous 0.1% (w/v) poly-L-lysine solution (Sigma-Aldrich GmbH, Munich, Germany) and covered by a coverslip. Images were taken on a Zeiss Axioplan 2 imaging microscope equipped with an AxioCam MRm camera and a Plan-Apochromat 100×, 1.40 Oil DIC oil-immersion objective. The exposure time was 500 ms. Digital images were acquired and analyzed with AxioVision 4.6 software (Zeiss, Göttingen, Germany).

Fluorescence-Activated Cell Sorting. Flow cytometric measurements were performed with a FACSAria II (Becton Dickinson, San Jose, USA) with 488 nm excitation (blue solid-state laser). Forward-scatter characteristics (FSC) and side-scatter characteristics (SSC) were detected as small-angle and large-angle scatters of the 488 nm laser, respectively. eYFP fluorescence was detected using a 502 nm long-pass and a 530/30 nm band-pass filter set. Data were analyzed using BD DIVA 6.1.3 software. The sheath fluid was sterile-filtered phosphate-buffered saline (137 mM NaCl, 2.7 mM KCl, 10 mM Na_2HPO_4, and 1.8 mM KH_2PO_4). Electronic gating was set to exclude nonbacterial particles on the basis of forward- versus side-scatter area. For sorting eYFP-positive cells, the next level of electronic gating was set to exclude nonfluorescent cells. Background was estimated using cells with pSenSox (wild-type *Lb*Adh) for sorting eYFP-positive cells. For screening cells having increased Adh activity with the substrate 4M2P, *E. coli* DH5α was transformed with a pSenSox library containing either site-directed or randomly mutagenized, via ep-PCR, *Lbadh*. After transformation, plating on LB agar plates containing ampicillin, and incubation for 18 h at 37 °C, the colonies were resuspended in 10 mL of 2× YT medium and diluted by a factor of 10 using 2× YT medium. Cells containing nonmutagenized pSenSox were used as background control. After 4 h of growth at 37 °C and 130 rpm, 20 mM 4M2P was added to the cells, and incubation was continued for 2.5 h, after which the cells were subjected to FACS.

Determination of Alcohol Dehydrogenase Activity. *E. coli* strains carrying the desired plasmids were cultured for 5 h at 37 °C and 130 rpm in 50 mL of 2× YT medium. Cells were harvested by centrifugation for 5 min at 10 000*g* and 4 °C. The cells were resuspended in 100 mM potassium phosphate buffer, pH 6.5, with 1 mM dithiothreitol and 1 mM $MgCl_2$. Cells were disrupted at 4 °C by 3 × 15 s bead-beating with glass beads (diameter 0.1 mm) using a Silamat S5 (Ivoclar Vivadent GmbH, Germany), and crude extracts were centrifuged for 20 min at 16 000*g* and 4 °C to remove intact cells and cell debris. The supernatants were used as cell-free extracts. Adh activity was measured photometrically at 340 nm using different dilutions of the cell-free extract using a mixture of 10 mM MAA, 250 μM NADPH, and 1 mM $MgCl_2$ in 100 mM potassium phosphate buffer, pH 6.5. Reactions were started by addition of cell-free extract. One unit of enzyme activity was defined as the amount of enzyme catalyzing the oxidation of 1 μmol min^{-1} NADPH at 30 °C under the specified conditions. Protein concentrations were determined by the method of Bradford[45] using bovine serum albumin as the standard. For the determination of the K_m values, substrate 4M2P was used at concentrations of 0.1−10 mM. K_m and V_{max} values were calculated using Lineweaver−Burk plots of the experimental data.[46]

■ ASSOCIATED CONTENT

Supporting Information

This material is available free of charge via the Internet at http://pubs.acs.org.

■ AUTHOR INFORMATION

Corresponding Author

*Phone: +49 2461 613294; Fax: +49 2461 612710; E-mail: m.bott@fz-juelich.de.

Present Address

[†]Technical University of Denmark, Novo Nordisk Foundation Center for Biosustainability, Kogle Allé 6, DK-2970 Hørsholm, Denmark.

Author Contributions

S.S., G.S., and S.Bi. performed the experiments, S.Br., L.E., and M.B. provided guidance for the experimental setups, and S.Br., L.E., and M.B. wrote the paper.

Notes

The authors declare no competing financial interest.

■ ACKNOWLEDGMENTS

We thank Alexander Grünberger for taking the epifluorescence pictures of the cells. This work was supported by the Ministry of Innovation, Science, Research and Technology of North Rhine-Westphalia (BioNRW, Technology Platform Biocatalysis, RedoxCell, support code W0805wb001b).

■ REFERENCES

(1) McDonald, A. G., Boyce, S., and Tipton, K. F. (2009) ExplorEnz: The primary source of the IUBMB enzyme list. *Nucleic Acids Res. 37*, D593−D597.

(2) Hall, M., and Bommarius, A. S. (2011) Enantioenriched compounds via enzyme-catalyzed redox reactions. *Chem. Rev. 111*, 4088−4110.

(3) Bornscheuer, U. T., Huisman, G. W., Kazlauskas, R. J., Lutz, S., Moore, J. C., and Robins, K. (2012) Engineering the third wave of biocatalysis. *Nature 485*, 185−194.

(4) Reetz, M. T. (2011) Laboratory evolution of stereoselective enzymes: A prolific source of catalysts for asymmetric reactions. *Angew. Chem., Int. Ed. 50*, 138−174.

(5) Huisman, G. W., Liang, J., and Krebber, A. (2010) Practical chiral alcohol manufacture using ketoreductases. *Curr. Opin. Chem. Biol. 14*, 122−129.

(6) Schroer, K., Mackfeld, U., Tan, I. A., Wandrey, C., Heuser, F., Bringer-Meyer, S., Weckbecker, A., Hummel, W., Daussmann, T., Pfaller, R., Liese, A., and Lütz, S. (2007) Continuous asymmetric ketone reduction processes with recombinant *Escherichia coli*. *J. Biotechnol. 132*, 438−444.

(7) Hummel, W. (1999) Large-scale applications of NAD(P)-dependent oxidoreductases: Recent developments. *Trends Biotechnol. 17*, 487−492.

(8) Ernst, M., Kaup, B., Müller, M., Bringer-Meyer, S., and Sahm, H. (2005) Enantioselective reduction of carbonyl compounds by whole-cell biotransformation, combining a formate dehydrogenase and a (*R*)-specific alcohol dehydrogenase. *Appl. Microbiol. Biotechnol. 66*, 629−634.

(9) Schlieben, N. H., Niefind, K., Müller, J., Riebel, B., Hummel, W., and Schomburg, D. (2005) Atomic resolution structures of *R*-specific alcohol dehydrogenase from *Lactobacillus brevis* provide the structural bases of its substrate and cosubstrate specificity. *J. Mol. Biol. 349*, 801−813.

(10) Greenberg, J. T., Monach, P., Chou, J. H., Josephy, P. D., and Demple, B. (1990) Positive control of a global antioxidant defense regulon activated by superoxide-generating agents in *Escherichia coli*. *Proc. Natl. Acad. Sci. U.S.A. 87*, 6181−6185.

(11) Tsaneva, I. R., and Weiss, B. (1990) *soxR*, a locus governing a superoxide response regulon in *Escherichia coli* K-12. *J. Bacteriol. 172*, 4197−41205.
(12) Wu, J., and Weiss, B. (1991) Two divergently transcribed genes, *soxR* and *soxS*, control a superoxide response regulon of *Escherichia coli*. *J. Bacteriol. 173*, 2864−2871.
(13) Amabile-Cuevas, C. F., and Demple, B. (1991) Molecular characterization of the *soxRS* genes of *Escherichia coli*: Two genes control a superoxide stress regulon. *Nucleic Acids Res. 19*, 4479−4484.
(14) Chiang, S. M., and Schellhorn, H. E. (2012) Regulators of oxidative stress response genes in *Escherichia coli* and their functional conservation in bacteria. *Arch. Biochem. Biophys. 525*, 161−169.
(15) Imlay, J. A. (2013) The molecular mechanisms and physiological consequences of oxidative stress: Lessons from a model bacterium. *Nat. Rev. Microbiol. 11*, 443−454.
(16) Watanabe, S., Kita, A., Kobayashi, K., and Miki, K. (2008) Crystal structure of the [2Fe-2S] oxidative-stress sensor SoxR bound to DNA. *Proc. Natl. Acad. Sci. U.S.A. 105*, 4121−4126.
(17) Hidalgo, E., and Demple, B. (1994) An iron-sulfur center essential for transcriptional activation by the redox-sensing SoxR protein. *EMBO J. 13*, 138−146.
(18) Ding, H., Hidalgo, E., and Demple, B. (1996) The redox state of the [2Fe-2S] clusters in SoxR protein regulates its activity as a transcription factor. *J. Biol. Chem. 271*, 33173−33175.
(19) Gaudu, P., and Weiss, B. (1996) SoxR, a [2Fe-2S] transcription factor, is active only in its oxidized form. *Proc. Natl. Acad. Sci. U.S.A. 93*, 10094−10098.
(20) Blanchard, J. L., Wholey, W. Y., Conlon, E. M., and Pomposiello, P. J. (2007) Rapid changes in gene expression dynamics in response to superoxide reveal SoxRS-dependent and independent transcriptional networks. *PLoS One 2*, e1186-1−e1186-13.
(21) Koo, M. S., Lee, J. H., Rah, S. Y., Yeo, W. S., Lee, J. W., Lee, K. L., Koh, Y. S., Kang, S. O., and Roe, J. H. (2003) A reducing system of the superoxide sensor SoxR in *Escherichia coli*. *EMBO J. 22*, 2614−2622.
(22) Liochev, S. I., Benov, L., Touati, D., and Fridovich, I. (1999) Induction of the *soxRS* regulon of *Escherichia coli* by superoxide. *J. Biol. Chem. 274*, 9479−9481.
(23) Gu, M., and Imlay, J. A. (2011) The SoxRS response of *Escherichia coli* is directly activated by redox-cycling drugs rather than by superoxide. *Mol. Microbiol. 79*, 1136−1150.
(24) Liochev, S. I., and Fridovich, I. (2011) Is superoxide able to induce SoxRS? *Free Radical Biol. Med. 50*, 1813.
(25) Fujikawa, M., Kobayashi, K., and Kozawa, T. (2012) Direct oxidation of the [2Fe-2S] cluster in SoxR protein by superoxide: Distinct differential sensitivity to superoxide-mediated signal transduction. *J. Biol. Chem. 287*, 35702−35708.
(26) Liochev, S. I., and Fridovich, I. (1992) Fumarase C, the stable fumarase of *Escherichia coli*, is controlled by the *soxRS* regulon. *Proc. Natl. Acad. Sci. U.S.A. 89*, 5892−5896.
(27) Krapp, A. R., Humbert, M. V., and Carrillo, N. (2011) The *soxRS* response of *Escherichia coli* can be induced in the absence of oxidative stress and oxygen by modulation of NADPH content. *Microbiology 157*, 957−965.
(28) Kobayashi, K., and Tagawa, S. (1999) Isolation of reductase for SoxR that governs an oxidative response regulon from *Escherichia coli*. *FEBS Lett. 451*, 227−230.
(29) Siedler, S., Bringer, S., and Bott, M. (2011) Increased NADPH availability in *Escherichia coli*: Improvement of the product per glucose ratio in reductive whole-cell biotransformation. *Appl. Microbiol. Biotechnol. 92*, 929−937.
(30) Siedler, S., Bringer, S., Blank, L. M., and Bott, M. (2012) Engineering yield and rate of reductive biotransformation in *Escherichia coli* by partial cyclization of the pentose phosphate pathway and PTS-independent glucose transport. *Appl. Microbiol. Biotechnol. 93*, 1459−1467.
(31) Imlay, J. A., and Fridovich, I. (1991) Assay of metabolic superoxide production in *Escherichia coli*. *J. Biol. Chem. 266*, 6957−6965.
(32) Binder, S., Schendzielorz, G., Stäbler, N., Krumbach, K., Hoffmann, K., Bott, M., and Eggeling, L. (2012) A high-throughput approach to identify genomic variants of bacterial metabolite producers at the single-cell level. *Genome Biol 13*, R40-1−R40-12.
(33) Mustafi, N., Grünberger, A., Kohlheyer, D., Bott, M., and Frunzke, J. (2012) The development and application of a single-cell biosensor for the detection of L-methionine and branched-chain amino acids. *Metab. Eng. 14*, 449−457.
(34) Schendzielorz, G., Dippong, M., Grünberger, A., Kohlheyer, D., Yoshida, A., Binder, S., Nishiyama, C., Nishiyama, M., Bott, M., Eggeling, L. (2013) Taking control over control: Use of product sensing in single cells to remove flux control at key enzymes in biosynthesis pathways. *ACS Synth. Biol.* [Online early access], DOI: 10.1021/sb400059y, Published Online: July 5, 2013.
(35) Liang, J. C., Chang, A. L., Kennedy, A. B., and Smolke, C. D. (2012) A high-throughput, quantitative cell-based screen for efficient tailoring of RNA device activity. *Nucleic Acids Res. 40*, e154.
(36) Raser, J. M., and O'Shea, E. K. (2004) Control of stochasticity in eukaryotic gene expression. *Science 304*, 1811−1814.
(37) Tang, S. Y., Fazelinia, H., and Cirino, P. C. (2008) AraC regulatory protein mutants with altered effector specificity. *J. Am. Chem. Soc. 130*, 5267−5271.
(38) Tang, S. Y., and Cirino, P. C. (2011) Design and application of a mevalonate-responsive regulatory protein. *Angew. Chem., Int. Ed. 50*, 1084−1086.
(39) Binder, S., Siedler, S., Marienhagen, J., Bott, M., and Eggeling, L. (2013) Recombineering in *Corynebacterium glutamicum* combined with optical nanosensors: A general strategy for fast producer strain generation. *Nucleic Acids Res. 41*, 6360−6369.
(40) Hanahan, D. (1983) Studies on transformation of *Escherichia coli* with plasmids. *J. Mol. Biol. 166*, 557−580.
(41) Miller, J. (1972) *Experiments in Molecular Genetics*, pp 352−355, Cold Spring Harbor Laboratory, Cold Spring Harbor, NY.
(42) Sambrook, J., and Russell, D. W. (2001) *Molecular Cloning: A Laboratory Manual*, 3rd ed., Cold Spring Harbor Laboratory Press, Cold Spring Harbor, NY.
(43) Wilson, D. S., and Keefe, A. D. (2001) Random mutagenesis by PCR, in *Current Protocols in Molecular Biology*, Chapter 8, Unit 8.3, Wiley, New York.
(44) Funke, M., Diederichs, S., Kensy, F., Müller, C., and Büchs, J. (2009) The baffled microtiter plate: Increased oxygen transfer and improved online monitoring in small scale fermentations. *Biotechnol. Bioeng. 103*, 1118−1128.
(45) Bradford, M. M. (1976) A rapid and sensitive method for the quantitation of microgram quantities of protein utilizing the principle of protein-dye binding. *Anal. Biochem. 72*, 248−254.
(46) Lineweaver, H., and Burk, D. (1934) The determination of enzyme dissociation constants. *J. Am. Chem. Soc. 56*, 658−666.